



# Decreasing predictability as a precursor indicator for abrupt climate change

Wenping He<sup>1,2,3</sup> · Xiaoqiang Xie<sup>1</sup> · Ying Mei<sup>1</sup> · Shiquan Wan<sup>4</sup> · Shanshan Zhao<sup>5</sup>

Received: 14 October 2020 / Accepted: 25 January 2021 / Published online: 6 February 2021  
© The Author(s), under exclusive licence to Springer-Verlag GmbH, DE part of Springer Nature 2021

## Abstract

Abrupt climate change has an important impact on sustainable economic and social development, as well as ecosystem. However, it is very difficult to predict abrupt climate changes because the climate system is a complex and nonlinear system. In the present paper, the nonlinear local Lyapunov exponent (NLLE) is proposed as a new early warning signal for an abrupt climate change. The performance of NLLE as an early warning signal is first verified by those simulated abrupt changes based on four folding models. That is, NLLE in all experiments showed an almost monotonous increasing trend as a dynamic system approached its tipping point. For a well-studied abrupt climate change in North Pacific in 1976/1977, it is also found that NLLE shows an almost monotonous increasing trend since 1970 which give up to 6 years warning before the abrupt climate change. The limit of the predictability for a nonlinear dynamic system can be quantitatively estimated by NLLE, and larger NLLE of the system means less predictability. Therefore, the decreasing predictability may be an effective precursor indicator for abrupt climate change.

**Keywords** Abrupt climate change · Tipping point · Nonlinear local Lyapunov exponent · Predictability · Early warning signal

## 1 Introduction

Abrupt climate change is an important and special form of climate change, which has an important impact on the ecological environment, sustainable economic and social development, and the extinction of species (Alley et al. 2003; Boers 2018; Clements et al. 2019; Roberts et al. 2019;

Rothman 2017). However, due to the human limited understanding of the climate system at present, it is still difficult for us to predict abrupt changes in the climate system using dynamical and statistical methods. Therefore, it is crucial to develop the theories and methods of early warning for abrupt climate change which will help us to monitor and warn of an impending abrupt change in the climate system or ecosystem in the future (Dakos et al. 2008; Lenton 2011; Scheffer et al. 2001).

In recent years, early warning of an abrupt climate change has become an international problem of great concern, as well as in other disciplines, including medicine, ecology, marine science, life science, seismology (Boulton et al. 2014; Clements and Ozgul 2016; Di Genova et al. 2017; Ding et al. 2016; Gottschalk et al. 2015; Henry et al. 2016; Klus et al. 2019; Liu et al. 2019; McSharry et al. 2003). Many kinds of early warning signals for abrupt change have been presented. For example, when a dynamic system approaches its tipping point, three early warning signals can be founded which can be explained by the phenomenon of critical slowing down, including slower recovery from perturbations, a marked increase in variance and autocorrelation (Carpenter and Brock 2006; Dakos et al. 2012; Scheffer et al.

✉ Wenping He  
wenping\_he@163.com

<sup>1</sup> School of Atmospheric Sciences, Sun Yat-sen University, and Key Laboratory of Tropical Atmosphere-Ocean System, Ministry of Education, and Southern Marine Science and Engineering Guangdong Laboratory (Zhuhai), Zhuhai 519082, China

<sup>2</sup> Collaborative Innovation Center on Forecast and Evaluation of Meteorological Disasters, Nanjing University of Information Sciences and Technology, Nanjing 210044, China

<sup>3</sup> LASG, Institute of Atmosphere Physics, Chinese Academy of Science, Beijing 100029, China

<sup>4</sup> Yangzhou Meteorological Office, Yangzhou 225009, China

<sup>5</sup> National Climate Center, Beijing 100081, China

2009). The changing skewness and kurtosis coefficient have also been proposed as an early warning signal for abrupt change in ecosystems (Guttal and Jayaprakash 2008; Xie et al. 2019a, b). Prettyman et al. (2018) introduced an indicator on the basis of the power spectrum (PS) and found that the indicator may be used to provide an early warning signal for anticipating tropical cyclones. Climate memory could increase the chance of abrupt climate change and has previously been used in anticipating a dynamical bifurcation in advance (Livina and Lenton 2007; van der Bolt et al. 2018). In addition, some other early warning signs have also been proposed, such as critical speeding up, eigenvalues of the covariance matrix, and self-organized patchiness (Chen et al. 2019; Titus and Watson 2020; Venegas et al. 2005). However, due to the complexity of the actual system, various methods have some flaws to some extent. For example, the autocorrelation function and climate memory can provide an effectively early warning for artificial data; however, they fail to warn the tropical cyclones (Prettyman et al. 2018). The skewness indicator as well as PS is found to fail to give an early warning in some artificial model (Guttal and Jayaprakash, 2008). So, it is still crucial to devise new indicator to effectively warn of an abrupt climate change.

Predictability usually refers to an upper limit on the timeliness of weather forecasting or climate prediction, and it is generally believed that predictability is mainly related to the uncertainty exist in climate model and the limited error of the initial conditions (Ding et al. 2008, 2015; Duan and Mu 2009; Hou et al. 2018; Huang and Fu 2019; Li and Ding 2013; Shukla and Gutzler 1983). In fact, the predictability of a system is also closely related to its dynamic characteristics (Ding et al. 2008). In view of this, the present study intends to investigate some general rules of the predictability of a dynamic system when the system approaches its tipping point, and then develop a new early warning indicator for abrupt climate change based on the predictability of the climate system.

The remainder of this paper is organized as follows. In Sect. 2, the algorithm of nonlinear local Lyapunov exponent (NLLE) is briefly described, and then four folding models and data used in this study are also presented. In Sect. 3, the performance of NLLE as an early warning signal is validated in artificial time series and North Pacific sea-level pressure records. The conclusions and discussion are provided in Sect. 4.

## 2 Method and models

### 2.1 Nonlinear local Lyapunov exponent

Most of traditional theories and methods of the predictability are designed based on the tangent linear model. However,

the climate system is a complex and nonlinear dynamic system. Thus, the traditional methods of the predictability have some limitations in dealing with nonlinear problems. To make up for the shortcomings of the existing theories and methods of the predictability, NLLE is presented based on the theoretical saturation level of error growth, and then the limit of predictability for a nonlinear dynamic system can be quantitatively estimated (Ding et al. 2008; Li and Ding 2011, 2013). Here, we briefly describe the algorithm of NLLE. A nonlinear dynamic system can be described as follows (Eq. (1)):

$$\frac{d}{dt}\mathbf{x} = \mathbf{F}(\mathbf{x}). \quad (1)$$

In Eq. (1),  $\mathbf{F}$  stands for mathematical operator of the nonlinear system, and the state vector is denoted by  $\mathbf{x}$ , namely,  $\mathbf{x} = [x_1(t), x_2(t), \dots, x_n(t)]^T$ . For a given initial error superimposed on a state  $\mathbf{x}$ ,  $\boldsymbol{\delta} = [\delta_1(t), \delta_2(t), \dots, \delta_n(t)]^T$ , the dynamic equation of the error can be written as follows (Eq. (2)):

$$\frac{d}{dt}\boldsymbol{\delta} = \mathbf{J}(\mathbf{x})\boldsymbol{\delta} + \mathbf{G}(\mathbf{x}, \boldsymbol{\delta}). \quad (2)$$

Here,  $\mathbf{J}(\mathbf{x})$  is obtained by tangent linear approximation to the error  $\boldsymbol{\delta}$ , and the function  $\mathbf{G}(\mathbf{x}, \boldsymbol{\delta})$  are the nonlinear terms. Traditionally, linear approximations are used to solve nonlinear problem, which usually assume that the tangent linear model of the error  $\boldsymbol{\delta}$  could be used to describe approximately the error evolution equation with sufficiently small initial perturbations. This linear approximation obviously has inherent limitations. To deal with the nonlinear problem of the error growth, NLLE is developed which does not need to conduct a linear approximation. Based on NLLE, the solutions of the dynamic equation of the error can be written as follows (Eq. 3):

$$\boldsymbol{\delta}_1 = \boldsymbol{\eta}(\mathbf{x}_0, \boldsymbol{\delta}_0, \tau)\boldsymbol{\delta}_0. \quad (3)$$

Here,  $\tau$  is the length of time of the error evolution, and  $\boldsymbol{\eta}(\mathbf{x}(t_0)\boldsymbol{\delta}(t_0), \tau)$  is the nonlinear error propagation operator. Thus, NLLE can be written mathematically as Eq. (4).

$$\lambda(\mathbf{x}_0, \boldsymbol{\delta}_0, \tau) = \frac{1}{\tau} \ln \frac{\|\boldsymbol{\delta}_1\|}{\|\boldsymbol{\delta}_0\|}. \quad (4)$$

In Eq. (4),  $\lambda(\mathbf{x}_0, \boldsymbol{\delta}_0, \tau)$  is a function of the initial error  $\boldsymbol{\delta}_0$  and evolution time  $\tau$  as well as the initial state  $\mathbf{x}_0$ . Based on this, we used NLLE to quantitatively estimate the predictability of a dynamic system in this study.

In this study, we defined a standardized NLLE as follows,

$$\text{Standardized NLLE} = \sum_{i=1}^N \frac{\lambda(\mathbf{x}_i, \boldsymbol{\delta}_0, \tau) - \bar{\lambda}}{\sigma}, i = 1, 2, 3 \dots, N. \quad (5)$$

In the Eq. (5),  $\bar{\lambda}$  is the mean of the series of the  $\lambda(x_i, \delta_0, \tau)$ , and  $\sigma$  is the standard deviation of the NLLE.

### 2.2 Models and data

Many dynamic systems in nature can exhibit a folding bifurcation. For example, with the increase of a surface fresh water perturbation in North Atlantic, Atlantic Meridional Overturning Circulation could be interrupted abruptly in a way of a folding bifurcation (Boulton, 2014). Some well-studied examples of abrupt change include ecological systems, coral reefs, lake eutrophication, financial crises, climate system, Arctic sea ice, and so on (Fraedrich 1978; Guttal and Jayaprakash 2008; Knowlton 1992; Steele 1996; Scheffer et al. 2001, 2009; Daskalov et al. 2007; Diks et al. 2019), and all of them can present a classical folding bifurcation. Therefore, it is importance to investigate the general rules before a dynamic system approach its critical points in such folding bifurcations.

In this study, a generalized logistic equation is first used to test the performance of NLLE as a new early warning indicator for an abrupt change. The generalized logistic equation is a one-dimensional model which is often used to describe the evolution of vegetation system. The model can be written mathematically as follows (Guttal and Jayaprakash 2008).

$$\frac{dV}{dt} = rV \left( 1 - \frac{V}{K} \right) - c \frac{V^2}{V^2 + V_0^2} + \sigma_V \eta_V(t). \tag{6}$$

In Eq. (6),  $V$  is the biomass density of the vegetation system, and  $K$  is a parameter which represents the carrying capacity of environment and is kept as a constant of 10 in our study. The parameter  $r$  is the growth rate of vegetation, which is a constant with a value of  $r=1$ . The maximum grazing rate is denoted by the parameter  $c$ , which ranges from 1 to 3. The parameter  $V_0$  is 1 in this study.  $\eta_V(t)$  is a stochastic variable, and  $\sigma_V$  is the standard deviation of the stochastic variable which ranges from 0 to 1:

$$\langle \eta_V(t) \eta_V(t') \rangle = \delta(t - t'). \tag{7}$$

Another vegetation model used in this study is two-dimensional stochastic differential equations, which is often used to simulate the affection of the rainfall rate on the vegetation biomass density in a semi-arid region (Guttal and Jayaprakash 2008; Xie et al. 2019a, b). This model is presented in Eqs. (8–9).

$$\frac{dw}{dt} = R - \alpha w - \lambda w B + \sigma_w \eta_w(t) \tag{8}$$

$$\frac{dB}{dt} = \rho B \left( w - \frac{B}{B_c} \right) - \mu \frac{B}{B + B_0} + \sigma_B \eta_B(t). \tag{9}$$

The parameter  $R$  is rainfall rate, and the variables  $w$  and  $B$  are the vegetation biomass density, soil water, respectively. The value of each parameter in the second model is shown

**Table 1** Description of parameters in Eq. (13)

Parameters	Values and physical meaning of parameters
$c$	A constant thermal inertia, $c=0.05$
$\epsilon$	Effective emissivity, $\epsilon = 0.69$
$\sigma$	Stefan Boltzmann constant, $\sigma = 5.67 \times 10^{-8}$
$\sigma_T$	The standard deviation of external noise, $\sigma_T = 0.003$
$\eta_T$	Uncorrelated Gaussian noise, <i>i.e.</i> $\langle \eta_T(t) \eta_T(t') \rangle = \delta(t - t')$
$I_0$	The solar constant, $I_0=1360$
$b$	A linear feedback between albedo and temperature, $b=0.009$
$a$	A linear feedback between temperature and ice, $a=2.8$

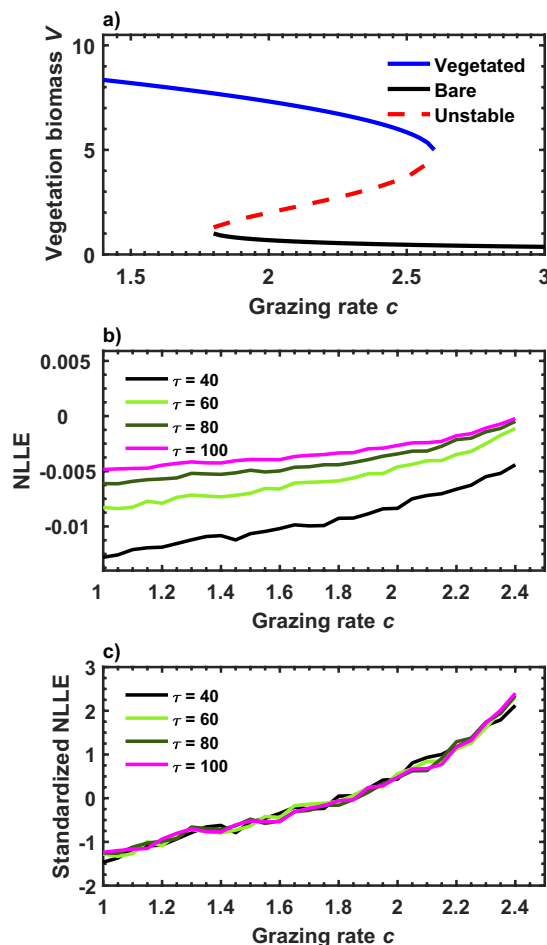


**Fig. 1** The NLLE results for one-dimensional ecosystem model. **a** The bifurcation diagram for the generalized logistic model (Eq. (6)); **b** NLLE as a function of the grazing rate  $c$  when the ecosystem approaches the tipping point of  $c^*=2.6$  for different evolutionary times; **c** same to Fig. 1b, but for the standardized NLLE.

here:  $\alpha = 1.0$ ,  $\lambda = 0.12$ ,  $\rho = 1$ ,  $B_c = 10$ ,  $\mu = 2$ , and  $B_0 = 1$ .  $\eta_w$  and  $\eta_B$  are two stochastic variable with the standard deviation  $\sigma_w$  and  $\sigma_B$ , respectively.

$$\frac{dP}{dt} = l - (h + s)P + [r + \sigma_r \eta_r(t)]MR(P) + \sigma_l \eta_l(t) \tag{10}$$

$$\frac{dM}{dt} = sP - bM - [r + \sigma_r \eta_r(t)]MR(P). \tag{11}$$

$$R(P) = \frac{P^q}{P_0^q + P^q} \tag{12}$$

Equations (10–12) are often used to simulate the eutrophication process of lakes (Guttal and Jayaprakash, 2008). Phosphorus concentrations in water and sediments are denoted by the two variables  $P$  and  $M$ , respectively. The parameter nutrient  $l$  is input rate which can vary from 0.5 to 1.0.  $\eta_l$  and  $\eta_r$  are two stochastic variables which can be used to describe the uncertainty of phosphorus uptake in water and sediments. The standard deviations of the two stochastic variable are both 0.01, namely,  $\sigma_l = 0.01$  and  $\sigma_r = 0.01$ . The values of the remaining parameters in the lake model are provided as follows:  $h = 0.15$ ,  $s = 0.7$ ,  $r = 0.019$ ,  $b = 0.001$ ,  $P_0 = 2.4$ , and  $q = 8$ . More detailed describes about those parameters in the above three models can be found in the literature (Guttal and Jayaprakash 2008).

The climate model is a simplified climate system which can be used to investigate the effect of infrared emission and solar heat input on the global average surface temperature. The geometrical dimension of the climate system is zero in the model, and thus Fraedrich (1978) called it a zero-dimensional climate model. The stochastic differential model is provided in Eq. (13).

$$\frac{dT}{dt} = \frac{1}{c} \left\{ -\varepsilon \sigma (T + \sigma_T \eta_T)^4 + \frac{1}{4} \mu I_0 b (T + \sigma_T \eta_T) + \frac{1}{4} \mu I_0 (1 - a) \right\}. \tag{13}$$

The average temperature  $T$  is subjected to radiative heating in Eq. (13). The parameter  $\mu$  ranges from 0.963 to 1 which is the relative radiative forcing. Table 1 provides the parameters in this model, and more detailed description of the climate model can be found in the literature (Fraedrich 1978).

Itô formula and Euler algorithm are used to numerically solve stochastic differential models. In order to examine the stability of the performance of NLLE, we study the ensemble mean of NLLE of the 100 time series obtained from an identical stochastic dynamic model with an identical set of parameters. Furthermore, we consider a well-studied abrupt climate change in North Pacific which is an observed interdecadal climate changes (Trenberth 1990). In order to determine whether NLLE of a time series can exhibit some general characteristics prior to an abrupt change in

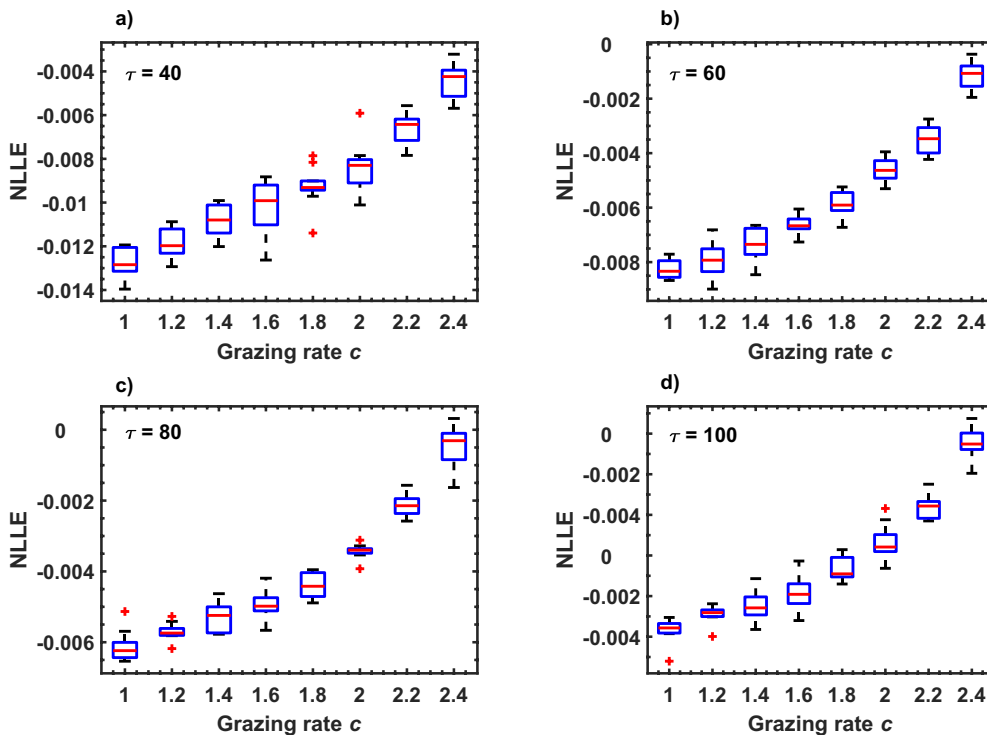


**Fig. 2** The box charts of NLLE for such 100 experiments for different lengths of time of the error evolution in the tests shown in Fig. 1b. **a** The lengths of time of the error evolution,  $\tau = 40$ ; **b**  $\tau = 60$ ; **c**  $\tau = 80$ ; and **d**  $\tau = 100$ .

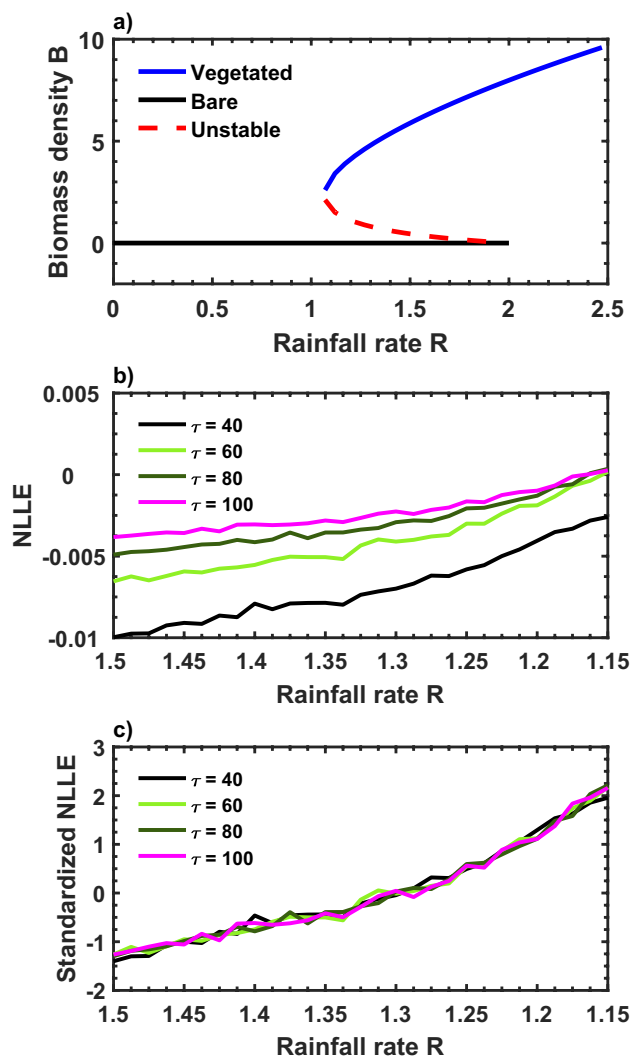


**Fig. 3** The NLLE results for the two-dimensional stochastic model. **a** The bifurcation diagram for the two-dimensional stochastic model; **b** the NLLE as a function of the rainfall rate  $R$  when the vegetation model approaches the tipping point of  $R^* = 1.06$  for different evolutionary times; **c** same to Fig. 3b, but for the standardized NLLE.

observational data, we applied NLLE to analyze the monthly North Pacific sea-level pressure records (<https://rda.ucar.edu/datasets/ds010.1/>).

### 3 Results

Many nonlinear models for oceanic circulation (e.g., Atlantic Meridional Overturning Circulation) and climate model often show folding bifurcations (Boulton et al. 2014; Fraedrich 1978). So, it is an effective way to use some simplified models to check the performance of a new early warning signal. On the basis of this, four simple folding models are firstly used to verify the effectiveness of NLLE as a new

early warning indicator for an abrupt change. The bifurcation diagram of the one-dimensional vegetation model is shown in Fig. 1a. Two tipping points of the vegetation model are  $c^* = 1.8$ , and 2.6, respectively. For  $c < 1.8$ , the system is in vegetated state, and a bare state will occur for  $c > 2.6$ . A bistable state will exist for  $1.8 < c < 2.6$ . Thus, the vegetated state and bare state could be interchanged abruptly when the vegetation system crosses one of the two tipping points.

First, a classic case of abrupt change is considered, namely, we linearly increase the grazing rate  $c$  at a very slow speed so that the vegetation system gradually approaches the critical tipping point ( $c^* = 2.6$ ). In this case, other parameters in this model are kept unchanged, and the 2000 time units for the first folding models were used to calculate the NLLE. In tests, the drift rate of the grazing rate  $c$  is 0.05. It is found that NLLE shows an almost monotonous increasing trend for different evolution times used for estimating NLLE as the grazing rate  $c$  approaches the tipping point ( $c^* = 2.6$ ) (Fig. 1b). In order to compare the trend of NLLE under different evolution times, NLLE is standardized. The results indicate that all of the standardized NLLE present an almost consistent evolutionary trend for different evolution times (Fig. 1c). The box charts of NLLE are also presented in Fig. 2 for such 100 experiments for different lengths of time of the error evolution. It can be found that the computed NLLE shows some relatively small fluctuations (Fig. 2). However, the overall increasing trend has been maintained before the system approaches its tipping point. It means that the increasing NLLE can provide a precursor signal prior to an abrupt change in the one-dimensional vegetation system (Eq. (6)).

The two-dimensional stochastic model also shows a folding bifurcation (Fig. 3a). The two critical tipping points of the model are  $R^* = 1.06$  and  $R^* = 2.0$ , respectively. If the system crosses one of the critical points, and the state of the vegetation model will shift from a vegetated state to bare one, or shift from a bare state to a vegetated state. In this study, sample size used to calculate the NLLE is exactly the same as the first stochastic model, and the rainfall rate  $R$  ranges from 2.4875 to 1.1875 with the drift rate of 0.0075 in all of numerical tests. The rainfall rate  $R$  is linearly and slowly decreased along the upper branch of the bifurcation, and other parameters in the two-dimensional stochastic model are kept unchanged. It is found that NLLE of the vegetation model has shown an almost monotonous increasing trend for different evolution times when the two-dimensional vegetation model is far away from the critical threshold of the rainfall rate  $R^* = 1.06$  (Fig. 3b). This increasing trend is clearer for the standardized NLLE, namely, an almost consistent evolutionary trend can be found for different evolution times used to calculate NLLE (Fig. 3c). Figure 4 presents the box charts of NLLE for such 100 experiments for the four different lengths of time of the error evolution. The

computed NLE's fluctuations are relatively small, and all of them present an increasing trend before the second stochastic vegetation approaches its tipping point.

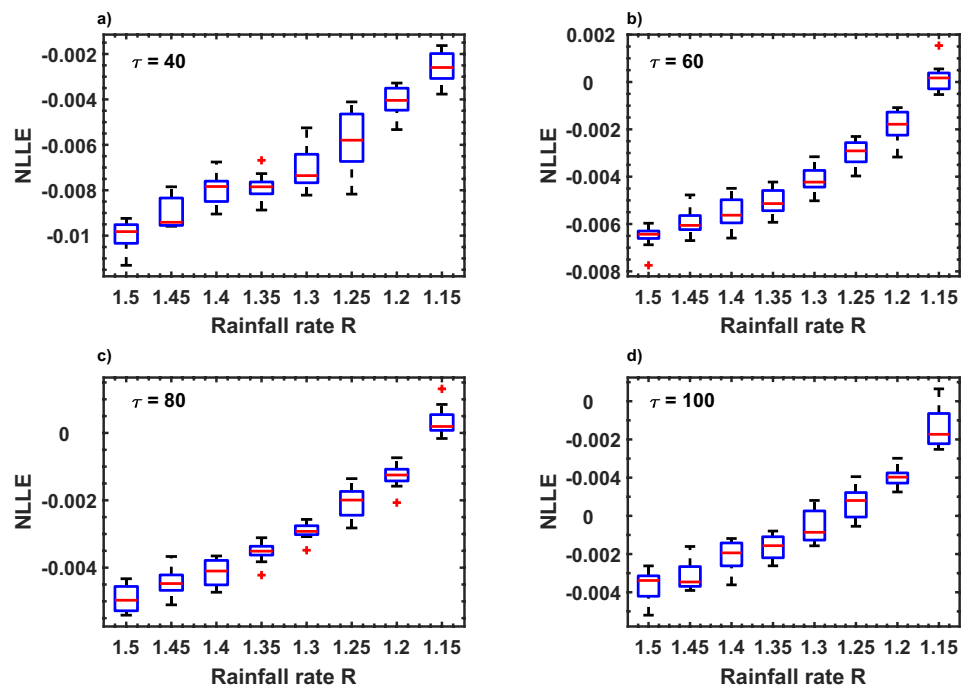
The stochastic lake model also showed a typical folding bifurcation (Fig. 5a). Two critical tipping points of the phosphorus loading rate are  $l^* = 0.5$  and  $l^* = 0.975$ , respectively. The lake system has two distinct states, namely, an oligotrophic state for  $l < 0.5$  and a eutrophic state for  $l > 0.975$ . The bistable state can occur for the lake system when the phosphorus loading rate  $l$  ranges from 0.5 to 0.975. If the lake system crosses its tipping point, the state will undergo an abrupt change between the two stable states. First, integrate this stochastic lake model for 7000 steps in the study with the integration step of 0.01. The initial values of the integration are  $M(t = 0) = 800$ , and  $P(t = 0) = 1$ , respectively. The first 1000 integral values are discarded as transient, and the phosphorus loading rate  $l$  ranges from 0.785 to 0.95 with the drift rate of 0.015. Along the lower branch of the bifurcation (Fig. 5a), we linearly increase the phosphorus loading rate  $l$  so that the lake system slowly approaches the tipping point of  $l^* = 0.975$ . The NLE of the time series of phosphorus concentrations shows a slow increasing trend before about  $l = 0.725$ , and then the increasing trend become significant (Fig. 5b). The standardized NLE obtained by different evolution times shows an almost consistent evolutionary trend which presents a more clearly increasing trend than that of NLE (Fig. 5c). Different from the previous two models' experimental results, the computed NLE based the stochastic lake model shows a relatively large fluctuations in

some cases for all four different lengths of time of the error evolution, including  $\tau = 40, 60, 80$ , and 100 (Fig. 6).

The geometrical dimension of the fourth stochastic model (Eq. (13)) used in this paper is zero, so it is usually called a zero-dimensional climate model. The simplified climate model can be used to simulate the energy flux balance between solar heat input and infrared emission from the globally averaged perspective. The solutions depend on the parameters in the climate model, and the relative radiative forcing  $\mu$  has an important effect on the average temperature  $T$ . The simplified climate model has two stable climatic states. If the relative radiative forcing  $\mu$  passes the tipping point ( $\mu^* = 0.97$ ), an interglacial climate will be interrupted and then abrupt shift to the "deep freeze" climate (Fraedrich 1978).

Figure 7a shows the average temperature  $T$  as a function of the relative radiative forcing  $\mu$ , and it is found that the average temperature  $T$  presents a diminishing trend with a decrease of the parameter  $\mu$ . A relatively warm climate was abruptly replaced by a cold climate when the average temperature  $T$  is decreased to the critical threshold of  $T^* = 266.67$  K at  $\mu^* = 0.97$  with the fixed drift of  $7.4 \times 10^{-6}$  (Fig. 7a). The integration step is 0.1 in the zero-dimensional climate model, and the sliding windows size used to calculate the NLE is 1000 data points. We found that NLE of the average temperature  $T$  presents an abruptly increasing trend prior to the abrupt change in the climate model (Fig. 7b). It means that NLE can provide an effective early warning signal for an upcoming abrupt climate change in the zero-dimensional climate model. It is worth pointing out that

**Fig. 4** Same to Fig. 2, but for the tests based on the second stochastic vegetation model, namely, the NLE as a function of the rainfall rate  $R$ . **a** The lengths of time of the error evolution,  $\tau = 40$ ; **b**  $\tau = 60$ ; **c**  $\tau = 80$ ; and **d**  $\tau = 100$ .



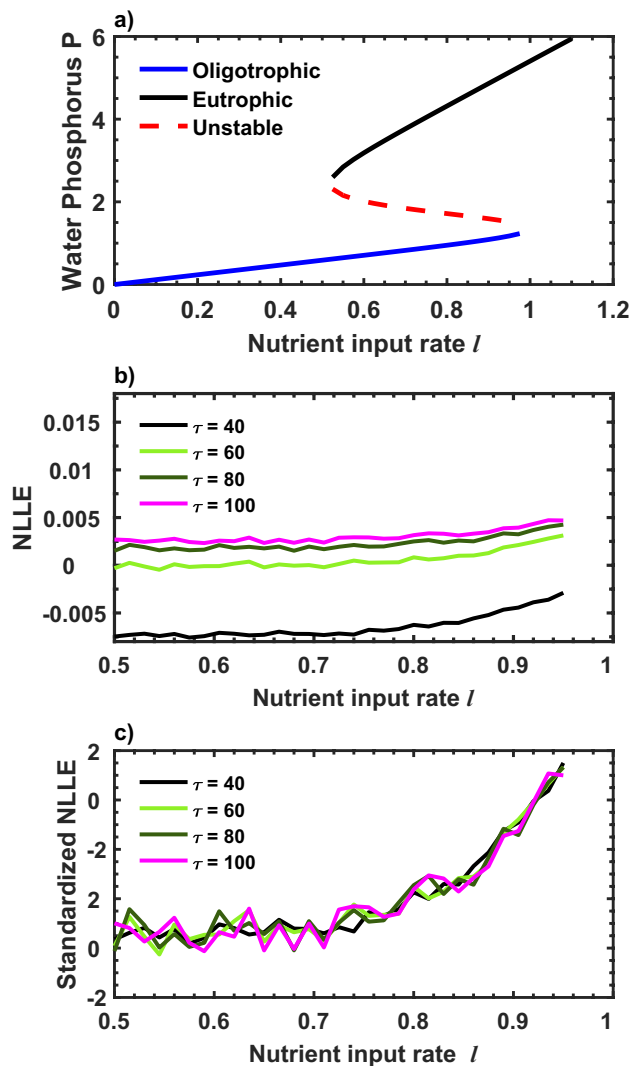


**Fig. 5** The NLLE results for the stochastic lake model. **a** The bifurcation diagram for lake model; **b** the NLLE as a function of the phosphorus loading rate  $l$  for different evolutionary times when the lake system approaches the critical threshold of  $l^* = 0.975$ ; **c** same to Fig. 5b, but for standardized NLLE

the increasing trend of NLLE does not seem obvious for a relatively short evolution time (e.g., evolution time  $\tau = 40$ ). However, the increasing trend in the standardized NLLE is almost the same for different evolution times (Fig. 7c).

Decadal shifts of the sea-level pressure are observed in North Pacific (Fraedrich 1978). Namely, there is an abrupt decreasing change after 1976 for North Pacific mean sea-level pressure for the winter period (Fig. 8a), averaged from  $27.5^\circ$  N to  $72.5^\circ$  N,  $147.5^\circ$  E to  $122.5^\circ$  W. The observed interdecadal climate changes in North Pacific provide a good test bed for determining if NLLE can provide an effective precursor signal prior to an abrupt climate change in observational data. We calculate the NLLE by using the North

Pacific mean sea-level pressure for the winter period during 1946 to 1976 which is prior to this abrupt climate change. The sliding windows size is 24 years in which the NLLE is estimated. For example, the NLLE of the winter sea-level pressure observed in North Pacific in 1960 can be calculated from 1946 to 1959. In order to investigate the influence of the length of time of the error evolution  $\tau$ , four different cases are considered in this study, including  $\tau = 2$  months, 4 months, 6 months, and 8 months. Figure 8b presents the time series of the standardized NLLE of North Pacific average sea-level pressure for the winter period. For all of four different lengths of time of the error evolution, an increasing trend of the standardized NLLE can be clearly identified and occurred around 1970 years which is far away from the time point of the interdecadal climate changes in North Pacific, 1976/1977.

## 4 Discussion and conclusions

At present, abrupt climate change is no longer just a subject of scientific research, and it has gradually become a major concern for society and government. Paleoclimate records such as ice cores, stalagmites, loess, lake deposits and spore-pollen have shown that an abrupt climate change is an indisputable fact (Alley et al. 2003), which can have some adverse effects on the ecological environment, and even lead to species extinction and dynasties subrogation. So, it has important scientific significance and application value to investigate the precursor signal for abrupt climate change. Based on several simple fold models, this study disclosed that during a dynamic system approaches its critical tipping point, NLLE will exhibit an increasing trend when the system is far away from its tipping point. Moreover, NLLE of the North Pacific sea-level pressure shows an obvious increasing trend from 1970 to 1976, which is prior to the abrupt climate change point of 1976/1977. The evolution time used to calculate NLLE has varying degrees of influence on the calculation of NLLE. However, the effect on the standardized NLLE is almost negligible which can be found from the results of the standardized NLLE. It indicates that changing NLLE can be used as a precursor signal of an upcoming abrupt climate change.

It is important to devise some new early warning signal because different indicators have different sources of uncertainty and limitations. NLLE is designed to quantitatively estimate the upper limit of predictability for a nonlinear dynamic system (Ding et al. 2008). Therefore, an important contribution of this study is that we found that the changing predictability may be an effective indicator for early warning of an abrupt climate change. We also explained why the predictability of a dynamic system can be regarded as an early warning signal for an abrupt change. As a dynamic system

**Fig. 6** Same to Fig. 2, but for the tests based on the stochastic lake model, namely, the NLE as a function of the phosphorus loading rate  $l$ . **a** The lengths of time of the error evolution,  $\tau = 40$ ; **b**  $\tau = 60$ ; **c**  $\tau = 80$ ; and **d**  $\tau = 100$ .

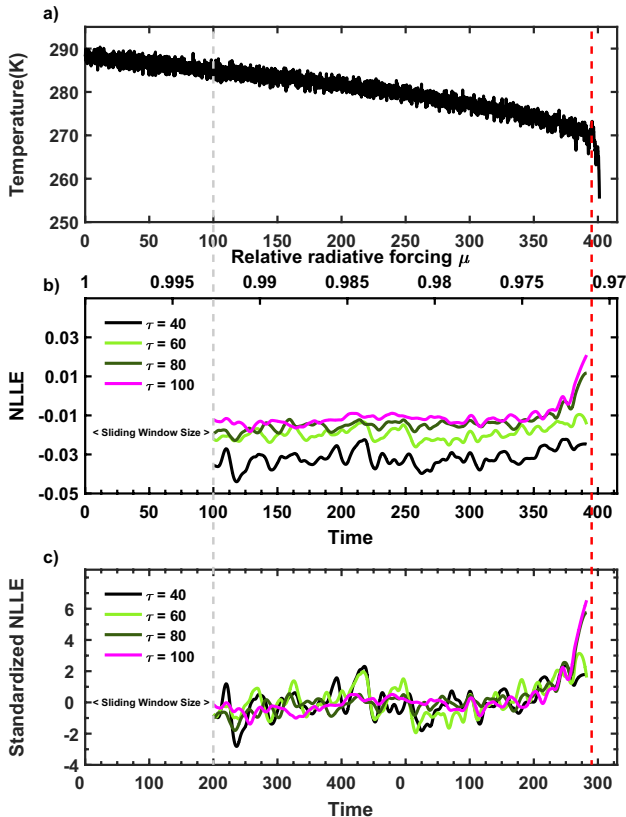
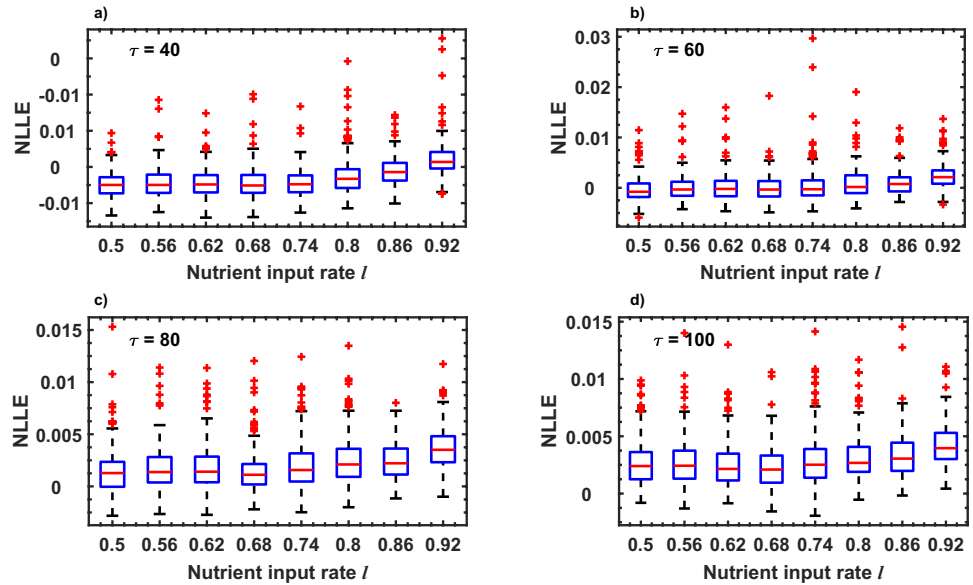


**Fig. 7** The NLE results for the zero-dimensional climate system. **a** The average temperature  $T$  as a function of the relative radiative forcing  $\mu$ ; **b** the NLE as a function of the relative radiative forcing  $\mu$  for different evolutionary times when the climate model approaches the tipping point of  $\mu^* = 0.97$ ; **c** same to Fig. 7b, but for the standardized NLE. Vertical red dashed line indicates the tipping point of  $\mu^* = 0.97$ . The top of the abscissa in Fig. 7 is the relative radiative forcing, and the bottom of the abscissa is time.

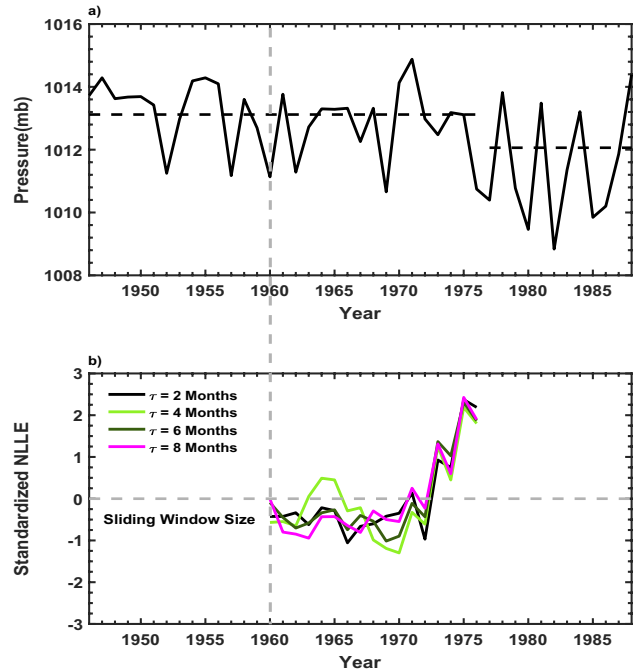


**Fig. 8** **a** The sea-level pressure in North Pacific averaged over  $27.5^\circ$  to  $72.5^\circ$  N,  $147.5^\circ$  E to  $122.5^\circ$  W from November to March. The dashed line indicates the means for 1946–1976 and 1977–1987, respectively; **b** the time series of the standardized NLE for the averaged sea-level pressure in North Pacific. The sliding windows size is 24 years in which the NLE is estimated.

approaches its tipping point, the stability of the system is gradually decreased and the instability increases. Thus, for the identical initial errors, a greater error growth rate would be found when the system is close to the tipping point, comparing that of the case when the system is far from the



tipping point. Therefore, the predictability of a system would be reduced as the dynamic system approaches its tipping point. Moreover, there are many quantitative estimation methods for the predictability of a dynamic system, such as signal-to-noise ratio (Shukla and Gutzler 1983; Li et al. 2013). Thus, one of future research works is to compare the performance of different estimation methods on predictability as a precursor signal of an abrupt climate change, as well as the influence of sample size, nonlinearity, and statistical significance of changing trends. The present study only considers a limited sample size to validate the performance of NMLE, and the dynamic system in nature may be more complicated than the folding model used in this study. So, more work is needed to find out how robust the NMLE indicator is in more complex dynamic systems. Moreover, the threshold to determine the warning time can be identified by abrupt change-point methods, and we will systematically study this problem in future work.

**Acknowledgements** This work was jointly supported by National Natural Science Foundation of China (Grant nos. 41775092, 41975086, 41875120, and 42075051), the Fundamental Research Funds for the Central Universities (Grant nos. 20lgzd06), LASG Open Research Program.

## Compliance with ethical standards

**Conflict of interest** The authors declare that they have no conflict of interest.

## References

- Alley RB, Marotzke J, Nordhaus WD et al (2003) Abrupt climate change. *Science* 299(28):2005–2010
- Boers N (2018) Early-warning signals for Dansgaard-Oeschger events in a high-resolution ice core record. *Nat Commun* 9:2556
- Boulton CA, Allison LC, Lenton TM (2014) Early warning signals of Atlantic Meridional Overturning Circulation collapse in a fully coupled climate model. *Nat Commun* 5:5752
- Carpenter SR, Brock WA (2006) Rising variance: a leading indicator of ecological transition. *Ecol Lett* 9:308–315
- Clements C, Ozgul A (2016) Including trait-based early warning signals helps predict population collapse. *Nat Commun* 7:10984. <https://doi.org/10.1038/ncomms10984>
- Clements CF, McCarthy MA, Blanchard JL (2019) Early warning signals of recovery in complex systems. *Nat Commun* 10:1681
- Chen S, O’Dea EB, Drake JM et al (2019) Eigenvalues of the covariance matrix as early warning signals for critical transitions in ecological systems. *Sci Rep* 9:2572
- Dakos V, Scheffer M, van Nes EH, Brovkin V, Petoukhov V, Held H (2008) Slowing down as an early warning signal for abrupt climate change. *Proc Natl Acad Sci USA* 105(38):14308–14312
- Dakos V, Carpenter SR, Brock WA, Ellison AM, Guttal V, Ives AR, Kéfi S, Livina V, Seekell DA, van Nes EH, Scheffer M (2012) Methods for detecting early warnings of critical transitions in time series illustrated using simulated ecological data. *PLoS One* 7:e41010
- Daskalov GM, Grishin AN, Rodionov S, Mihneva V (2007) Trophic cascades triggered by overfishing reveal possible mechanisms of ecosystem regime shifts. *Proc Natl Acad Sci USA* 104:10518–10523
- Di Genova D, Kolzenburg S, Wiesmaier S et al (2017) A compositional tipping point governing the mobilization and eruption style of rhyolitic magma. *Nature* 552:235–238
- Diks C, Hommes C, Wang J (2019) Critical slowing down as an early warning signal for financial crises? *Empir Econ* 57:1201–1228. <https://doi.org/10.1007/s00181-018-1527-3>
- Ding RQ, Li JP, Ha K (2008) Nonlinear local Lyapunov exponent and quantification of local predictability. *Chin Phys Lett* 25(5):1919–1922
- Ding RQ, Li J, Zheng F, Feng J, Liu DQ (2015) Estimating the limit of decadal-scale climate predictability using observational data. *Clim Dyn* 46(5):1563–1580
- Ding RQ, Li J, Tseng YH, Ha KJ, Zhao S, Lee JY (2016) Interdecadal change in the lagged relationship between the Pacific–South American pattern and ENSO. *Clim Dyn* 47:2867–2884
- Duan WS, Mu M (2009) Conditional nonlinear optimal perturbation: applications to stability, sensitivity, and predictability. *Sci China (D)* 52:884–906
- Fraedrich K (1978) Structural and stochastic analysis of a zero-dimensional climate system. *Q J R Meteorol Soc* 104:461–474
- Gottschalk J, Skinner LC, Misra S et al (2015) Abrupt changes in the southern extent of North Atlantic Deep Water during Dansgaard-Oeschger events. *Nat Geosci* 8:950–954
- Guttal V, Jayaprakash C (2008) Changing skewness: an early warning signal of regime shifts in ecosystems. *Ecol Lett* 11(5):450–460
- Henry LG, McManus JF, Curry WB, Roberts NL, Piotrowski AM, Keigwin LD (2016) North Atlantic ocean circulation and abrupt climate change during the last glaciation. *Science* 353(6298):470–474
- Hou ZL, Li JP, Ding RQ, Karamperidou C, Duan WS, Liu T, Feng J (2018) Asymmetry of the predictability limit of the warm ENSO phase. *Geophys Res Lett* 45(15):7646–7653
- Knowlton N (1992) Thresholds and multiple stable states in coral reef community dynamics. *Integr Comp Biol* 32:674
- Huang Y, Fu ZT (2019) Enhanced time series predictability with well-defined structures. *Theor Appl Climatol*. <https://doi.org/10.1007/s00704-019-02836-6>
- Klus A, Prange M, Varma V et al (2019) Spatial analysis of early-warning signals for a North Atlantic climate transition in a coupled GCM. *Clim Dyn* 53:97–113
- Lenton TM (2011) Early warning of climate tipping points. *Nat Clim Change* 1(4):201–209
- Li JP, Ding RQ (2011) Temporal–spatial distribution of atmospheric predictability limit by local dynamical analogues. *Mon Weather Rev* 139:3265–3283
- Li JP, Ding RQ (2013) Temporal–spatial distribution of the predictability limit of monthly sea surface temperature in the global oceans. *Int J Climatol* 33:1936–1947
- Li AB, Zhang LF, Wang QL et al (2013) Information theory in nonlinear error growth dynamics and its application to predictability: taking the Lorenz system as an example. *Sci China Earth Sci* 56:1413–1421
- Livina V, Lenton TM (2007) A modified method for detecting incipient bifurcations in a dynamical system. *Geophys Res Lett* 34:L03712
- Liu YL, Kumar M, Katul GG, Porporato A (2019) Reduced resilience as an early warning signal of forest mortality. *Nat Clim Change* 9:1–6
- McSharry PE, Smith LA, Tarassenko L (2003) Prediction of epileptic seizures: are nonlinear methods relevant? *Nat Med* 9:241–242
- Prettyman J, Kuna T, Livina V (2018) A novel scaling indicator of early warning signals helps anticipate tropical cyclones. *EPL* 121:10002

- Roberts CP, Allen CR, Angeler DG, Twidwell D (2019) Shifting avian spatial regimes in a changing climate. *Nat Clim Change* 9:562–566
- Rothman DH (2017) Thresholds of catastrophe in the Earth system. *Sci Adv* 3:e1700906
- Scheffer M, Carpenter SR, Foley JA, Folke C, Walker B (2001) Catastrophic shifts in ecosystems. *Nature* 413:591–596
- Scheffer M, Bascompte J, Brock WA, Brovkin V, Carpenter SR, Dakos V, Sugihara G (2009) Early-warning signals for critical transitions. *Nature* 461(7260):53–59
- Shukla J, Gutzler DS (1983) Interannual variability and predictability of 500 mb geopotential heights over the northern hemisphere. *Mon Weather Rev* 111:1273–1279
- Steele J (1996) Regime shifts in fisheries management. *Fish Res* 25:19–23
- Trenberth KE (1990) Recent observed interdecadal climate changes in the northern hemisphere. *Bull Am Meteorol Soc* 7:988–993
- Titus M, Watson J (2020) Critical speeding up as an early warning signal of stochastic regime shifts. *Theor Ecol*. <https://doi.org/10.1007/s12080-020-00451-0>
- van der Bolt B, van Nes EH, Bathiany S et al (2018) Climate reddening increases the chance of critical transitions. *Nat Clim Change* 8:478–484
- Venegas JG et al (2005) Self-organized patchiness in asthma as a prelude to catastrophic shifts. *Nature* 434:777–782
- Xie XQ, He WP, Gu B, Mei Y, Zhao SS (2019a) Can kurtosis be an early warning signal for abrupt climate change? *Clim Dyn* 52:6863–6876
- Xie XQ, He WP, Gu B, Mei Y, Wang JS (2019b) The robustness of the skewness as an early warning signal for abrupt climate change. *Int J Climatol*. <https://doi.org/10.1002/JOC.6179>

**Publisher's Note** Springer Nature remains neutral with regard to jurisdictional claims in published maps and institutional affiliations.